Eur. Phys. J. A **17**, 167–171 (2003)
DOI 10.1140/epja/i2003-10002-x

THE EUROPEAN PHYSICAL JOURNAL A

In-beam γ-ray spectroscopy of ^{190}Po: First observation of a low-lying prolate band in Po isotopes

K. Van de Vel[1,a], A.N. Andreyev[1,2], R.D. Page[2], H. Kettunen[3], P.T. Greenlees[3], P. Jones[3], R. Julin[3], S. Juutinen[3], H. Kankaanpää[3], A. Keenan[3], P. Kuusiniemi[3], M. Leino[3], M. Muikku[3,b], P. Nieminen[3], P. Rahkila[3], J. Uusitalo[3], K. Eskola[4], A. Hürstel[5], M. Huyse[1], Y. Le Coz[5], M.B. Smith[6,c], P. Van Duppen[1], and R. Wyss[7]

[1] Instituut voor Kern- en Stralingsfysica, University of Leuven, Belgium
[2] Oliver Lodge Laboratory, Department of Physics, University of Liverpool, UK
[3] Department of Physics, University of Jyväskylä, Finland
[4] Department of Physics, University of Helsinki, Finland
[5] DAPNIA/SPhN, CEA Saclay, France
[6] Department of Physics and Astronomy, Rutgers University, USA
[7] Department of Physics, Royal Institute of Technology, Stockholm, Sweden

Received: 10 January 2003 / Revised version: 19 February 2003 /
Published online: 7 May 2003 –
Communicated by J. Äystö

Abstract. Gamma rays from excited states of ^{190}Po have been observed using the Jurosphere Ge-detector array coupled to the RITU gas-filled separator. They were associated with a collective band which from spin $4\hbar$ onwards resembles the prolate rotational bands known in the isotones ^{188}Pb and ^{186}Hg. This indicates that in ^{190}Po the prolate configuration becomes yrast above $I = 2\hbar$. The experimental results are interpreted in a two-band mixing calculation and are in agreement with α-decay data and potential energy surface calculations.

PACS. 23.20.Lv Gamma transitions and level energies – 25.70.-z Low and intermediate energy heavy-ion reactions – 27.80.+w $190 \leq A \leq 219$ – 21.60.Ev Collective models

1 Introduction

Different shapes, coexisting at low excitation energies and interacting at low spin, form a well-established phenomenon in neutron mid-shell nuclei near $Z = 82$, see [1–4] and references therein. While the spherical shape is attributed to the $Z = 82$ shell closure, the deformed configurations have been associated with intruder states resulting from the excitation of one or more proton pairs across the $Z = 82$ shell gap.

The relative positions of the coexisting configurations in polonium isotopes have been calculated in Nilsson-Strutinsky calculations by May *et al.* [1] for axial symmetric shapes and by Oros *et al.* [2] taking into account both axial and non-axial shapes. The Po nuclei with $A > 194$ were calculated to have a near-spherical ground state reflecting the polarization effect of the valence proton pair. An oblate configuration was found to lower its energy with decreasing mass until in ^{192}Po the oblate minimum becomes lowest in energy.

These conclusions are supported by available experimental data obtained from complementary α/β-decay measurements (see [5–10] and references therein) and in-beam γ-ray spectroscopy (see [4,11] and references therein). For example, the excited oblate 0^+ intruder state in $^{196-202}$Po, observed in α- and β-decay studies [5], lowers its energy from 1757 keV in ^{202}Po to 567 keV in ^{196}Po. Alpha-decay studies of Po nuclei demonstrated that the decay strength to the oblate intruder state in the daughter Pb nuclei becomes larger compared to the feeding to the spherical ground state when moving towards the neutron mid-shell [7–9]. Alpha-decay mixing calculations suggest that the main component of the ground-state wave function of ^{192}Po is the oblate configuration [7,8]. The increase in collectivity when moving towards the neutron mid-shell becomes also clear from the low-energy level structure observed down to ^{192}Po as discussed in ref. [11] and references therein.

[a] e-mail: karen.vandevel@fys.kuleuven.ac.be
[b] *Present address*: Säteilyturvakeskus Laippatie, Helsinki, Finland.
[c] *Present address*: TRIUMF, 4004 Wesbrook Mall, Vancouver, B.C., Canada V6T 2A3.

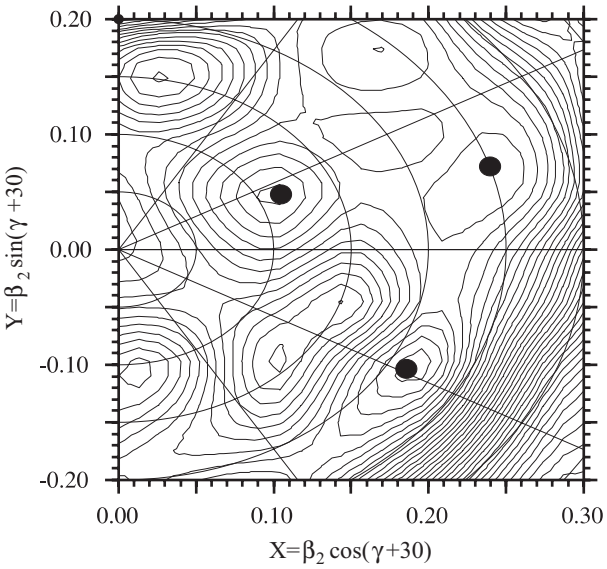

Fig. 1. Potential energy surface for ^{190}Po. The coexisting near-spherical, oblate and prolate minima are marked with dots. The distance between the contour lines is 50 keV.

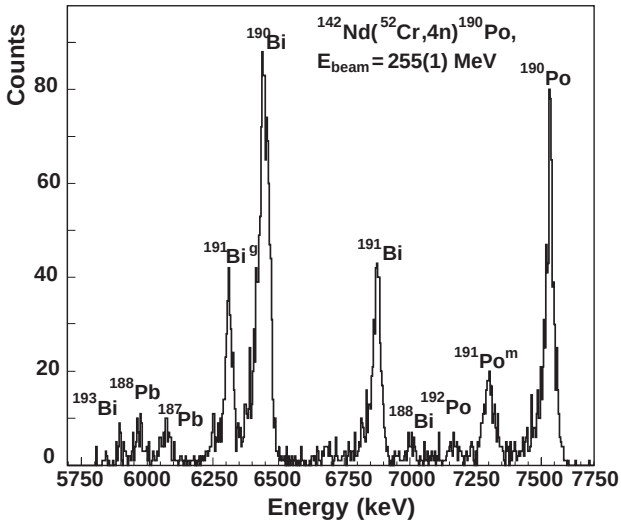

Fig. 2. The energy spectrum of α-particles correlated with recoils within 12 ms. Some α peaks are labeled with the nucleus they belong to.

In contrast to the Po nuclei with $A \geq 192$ where both calculations and experimental data show no evidence for the presence of a low-lying prolate configuration, the calculations of refs. [1,2] suggest the occurrence of triple shape coexistence at low energy for $N = 106$. The potential energy surface (PES) for ^{190}Po shown in fig. 1 was calculated using the formalism described in [2,12]. As in the neighbouring isotope ^{192}Po, the oblate ($|\beta_2| = 0.216$) minimum is predicted to lie lowest in energy in ^{190}Po, coexisting with a near-spherical ($|\beta_2| = 0.11$) minimum at ~ 40 keV. A prolate minimum with a relatively large prolate deformation ($|\beta_2| = 0.247$) appears at an excitation energy of only ~ 170 keV.

Experimental evidence for the presence of a prolate configuration was found in a recent α-decay study of ^{190}Po [9,10]. Evaluation of the hindrance factors for the fine-structure α-decay to the three coexisting 0^+ states in the daughter nucleus ^{186}Pb suggests that the ground state of ^{190}Po comprises a dominant oblate component, with prolate and near-spherical admixtures. The present in-beam study of ^{190}Po was performed in order to provide a better insight in the appearance of and consequent mixing between the low-lying prolate, oblate and near-spherical states.

2 Experimental details

Excited states in ^{190}Po were populated in the ^{142}Nd(^{52}Cr, 4n) reaction. The beam with an average intensity of about 12 pnA was delivered by the $K = 130$ MeV cyclotron at the Accelerator Laboratory of the University of Jyväskylä at a bombarding energy of 255 MeV. Prompt γ-rays emitted at the target position were measured by the Jurosphere Ge-detector array with an absolute photopeak efficiency of approximately 1.6% for 1.3 MeV γ-rays. The gas-filled recoil separator RITU [13] was used to separate recoiling fusion-evaporation products from beam particles and from the large fission background. The recoils were implanted into a 80 mm $\times$ 35 mm position-sensitive silicon strip detector (PSSD) in the focal plane. The detector consisted of 16 strips of 5 mm width, each position sensitive along the strip with a position resolution of 400 μm. A recently developed multi-wire proportional avalanche counter [14] was installed in front of the PSSD. Based on the different energy loss in this counter, it was possible to discriminate between scattered beam particles and recoils. Even more importantly, the anti-coincidence condition between the signals from the avalanche counter and the silicon detector allowed the recoil implantations and their subsequent α-decays in the PSSD to be distinguished, which resulted in clean α-particle spectra. For the implanted recoils and their α-decays the position, energy and time of detection in the strip detector was recorded. This information made it possible to use the recoil-decay tagging (RDT) technique [15] in which α-decays are time and position correlated with the detected recoils, and thus tag prompt γ-rays emitted by the recoils at the target position. More details on the method used can be found in [11].

3 Results

Figure 2 shows a part of the α-particle energy spectrum recorded in the PSSD in anti-coincidence with the signals from the avalanche counter. The α-decays were required to be preceded by the implantation of a recoil at the same position in the silicon detector within a time interval of 12 ms. A half-life value of 2.5(1) ms was deduced for the 7533(10) keV α line of ^{190}Po, which is consistent with the value of $T_{1/2} = 2.45(5)$ ms from [9].

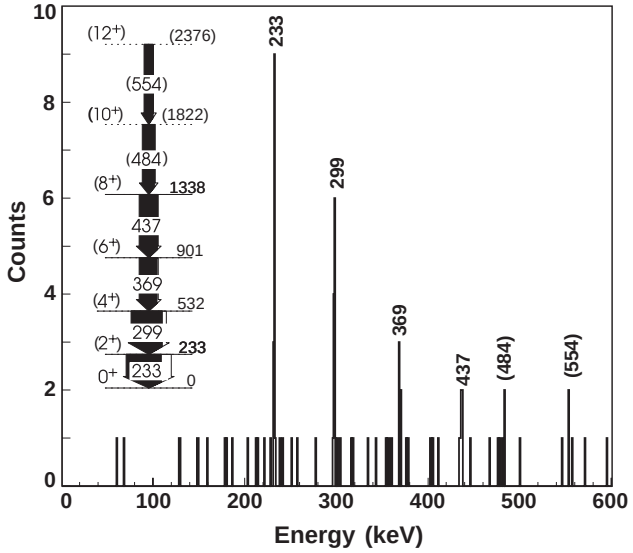

Fig. 3. γ-ray energy spectrum tagged with the α-decay of ^{190}Po (ΔT(recoil-α) $\leq$ 12 ms). The γ peaks are labeled with the decay energy (in keV). Insert: proposed level scheme for ^{190}Po; the energies are in keV. All spin assignments are tentative. The tentative 10^+ and 12^+ states are shown by dotted lines.

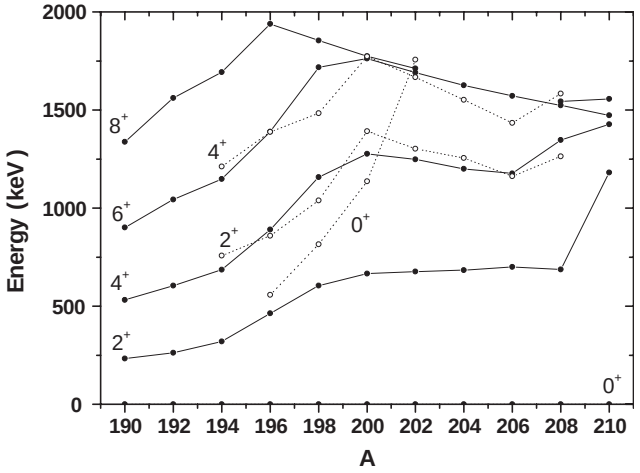

Fig. 4. Systematics of selected positive-parity near-yrast states for even-even polonium isotopes. Yrast states are indicated by filled circles, states with the same spin and parity are connected by a full line. The non-yrast levels, indicated with empty circles, are connected with a dotted line. The data are taken from refs. [11,16–21] and the present work.

From the alpha-particle counting rate and an estimate of the RITU transport efficiency of 35% the production cross-section for ^{190}Po was found to be $\approx$ 160 nb. The strongest fusion-evaporation channels lead to the production of ^{190}Bi (E_α = 6431, 6456 keV) and of ^{191}Bi (E_α = 6311 keV, $9/2^-$ isomer) with cross-section values of 20 μb, 6 μb, respectively.

Figure 3 shows the energy spectrum of γ-rays, resulting from the RDT analysis with a gate on the E_α = 7533(10) keV decay of ^{190}Po. Four γ-ray transitions are clearly identified in the γ-ray spectrum at 233 keV (13 counts), 299 keV (11 counts), 369 keV (5 counts), 437 keV (5 counts) with an accuracy of 1 keV and possibly two more at 484 keV (3 counts) and 554 keV (2 counts). The efficiency-corrected relative intensities of the 233, 299, 369, 437, 484 and 554 keV transitions are 100(20), 89(20), 52(25), 50(25), 35(20) and 26(20)%, respectively, the error includes both statistical and γ-ray detection efficiency uncertainties. Owing to the low statistics, no coincidences between the γ-rays were observed. Therefore, based on the level energy systematics for the heavier even-mass Po isotopes [4,11] and on the intensity pattern of the peaks, a tentative energy level scheme of ^{190}Po was deduced as shown in the inset to fig. 3.

4 Discussion

In order to explore the underlying structure of the observed states of ^{190}Po, its level structure has been compared with the level systematics of the heavier polonium isotopes and of the N = 106 isotones. Positive-parity near-yrast states up to 8^+ relevant for the discussion are shown fig. 4 for the even-mass $^{190-210}$Po isotopes. For polonium isotopes with 194 $\leq A \leq$ 208, second 2^+ and 4^+ states have been identified, together with excited 0^+ states in $^{196-202}$Po. Data are taken from refs. [5,11,16–21]. For ^{208}Po down to ^{200}Po, the rather constant energy behaviour of the yrast states has been described in the Particle Core Model (PCM), with the two valence protons coupled to a vibrating Pb core, by Younes and Cizewski in refs. [22,23] and by Oros *et al.* in [2]. While both groups reproduced the experimental yrast and second-excited 2^+ and 4^+ levels for $A \geq 200$, a sharp rise of the proton-core interaction parameter was introduced by the authors of [22,23] in order to describe the levels for $A \leq 198$. Oros *et al.* [2] argued against this unphysical sharp increase in the proton-core interaction strength. They concluded that one cannot describe the level energy systematics from ^{198}Po down to ^{192}Po using an anharmonic vibrator framework by keeping the PCM parameters in a physically meaningful range [2]. Furthermore, the trend of the excited 0^+ state could not be described within the PCM approach by both groups. Recent QRPA calculations for $^{192-210}$Po [24] predict 2^+ vibrational states to exhibit little collectivity and to have a nearly constant excitation energy of $\approx$ 1 MeV. The calculations give no sign for enhanced vibrational coupling when moving towards the neutron mid-shell. Therefore, the structure of the Po isotopes for $A \leq 198$ cannot be associated with enhanced collectivity of vibrational character.

On the other hand, the change in the low-energy level systematics of the polonium isotopes below ^{200}Po can be explained as the manifestation of shape coexistence at low excitation energy in the Po isotopes as discussed in refs. [2,4–6,11]. The fall in energy of the deformed configuration when moving towards the neutron mid-shell results in increasing mixing with the nearly spherical states. Consequently, the observed levels do not represent pure

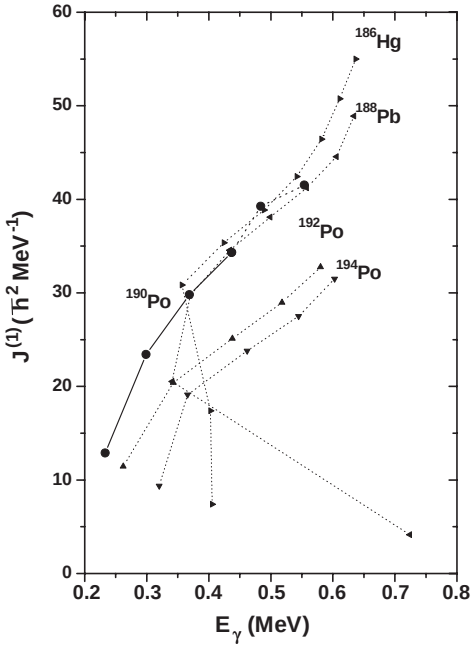

Fig. 5. Kinematic moment of inertia, as a function of γ-ray transition energy for the yrast band observed in ^{190}Po (circles), ^{192,194}Po (triangles up, triangles down, respectively) [11], and in the $N = 106$ isotones ^{188}Pb (left triangles) [25] and ^{186}Hg (right triangles) [26]. Tentative data for ^{190}Po (two last transitions) are shown by a dotted line.

configurations but comprise the coexisting components with contributions varying as a function of neutron number. In ^{198,196}Po the yrast states are of mainly near-spherical character with the non-yrast band of more collective character. The yrast band in ^{194,192}Po shows regularly increasing level spacings and has been associated with the oblate configuration [4,11]. The present level scheme of ^{190}Po shows a levelling-off of the 2^+ state, while the states from spin $4\hbar$ onwards drop further down in energy. This seems to indicate that another structure sets in ^{190}Po compared to the oblate configurations in ^{192,194}Po.

The difference between the level structure of ^{190}Po and ^{192,194}Po becomes also clear by plotting the kinematic moments of inertia, $J^{(1)}$, as a function of γ-ray transition energy. This is shown in fig. 5 for the yrast states in ^{190,192,194}Po, and in the $N = 106$ isotones ^{188}Pb and ^{186}Hg, data are taken from refs. [18,19,25,26]. For the polonium isotopes the $J^{(1)}$ values, and hence the collectivity, increase with decreasing neutron number. From spin 4^+ upwards, the observed rotational band in ^{190}Po has a moment of inertia which is nearly identical to those of the known prolate bands in the isotones ^{188}Pb and ^{186}Hg [25, 26]. This similarity suggests that the levels with $I^\pi \geq 4^+$ in ^{190}Po, ^{188}Pb and ^{186}Hg are based on the same structure: the prolate configuration. A variable moment of inertia (VMI) fit [27] using the energies of the 4^+ to 8^+ levels of ^{190}Po yields VMI parameters that are compatible with those extracted for ^{186}Hg and ^{188}Pb, and suggests that the unperturbed prolate 0^+ state lies at an excitation energy of only ~ 100 keV. Below spin $4\hbar$ the yrast band of ^{190}Po, ^{188}Pb and ^{186}Hg behaves irregularly as a result of crossing and mixing of different structures coexisting with different separation energy and mixing strengths.

In order to reproduce the collective bands associated with shape coexistence, a two-band (oblate-prolate) mixing calculation [28] has been performed. The VMI parameters of the bands were fixed to those extracted for ^{188}Pb (prolate band) and ^{192}Po (oblate band). This latter assumption is justified as the PES calculations predict a similar deformation parameter for the oblate configuration in ^{190,192,194}Po. The band head energies of the two bands and the spin-independent mixing strength parameter were determined by assuming different configurations for the experimentally observed levels with $I \geq 2\hbar$. By associating the states above $I = 4\hbar$ with the prolate configuration, and by taking the 2^+ level to be either of mainly oblate character or of mainly prolate character, the experimentally observed level energies for $I \geq 2\hbar$ could be fitted reasonably well. The unperturbed oblate 0^+ state was always found to lie below the unperturbed prolate 0^+ state; this ordering of the states was anticipated by the PES calculations. However, a discrepancy between the energy of the calculated mixed oblate 0^+ state and the experimentally observed ground state was found, with the mixed oblate level lying $\sim$ 40–90 keV higher in energy. Similar results were obtained using the oblate band parameters from ^{194}Po. A possible reason for the discrepancy between the energy of the calculated mixed oblate 0^+ state and the experimentally observed ground state could be the presence of a low-lying near-spherical configuration (see fig. 1), which through mixing with the oblate one, produces a ground state lower in energy. As was mentioned in the introduction, evidence for a small admixture of a spherical component in the ground-state wave function of ^{190}Po was deduced in [10] based on the analysis of the α-decay hindrance factors. The larger energy spacing of the spherical levels compared to the more deformed oblate and prolate structures implies that the higher-spin spherical levels will have a much more reduced effect on the deformed yrast (and non-yrast) states of the same spin. These data and their analysis may therefore be a preliminary indication of triple shape coexistence in ^{190}Po, as was identified in its daughter ^{186}Pb [9]. Further experiments to identify non-yrast (particularly 0^+) states are clearly required to establish whether this is indeed the case.

We note that the decrease of the prolate minimum with increasing spin is in agreement with total Routhian surface calculations which predict that the moment of inertia for the prolate shape is 30% larger than for the oblate shape [29]. Then according to the PES calculations the prolate configuration further drops down in energy, forming the main component of the ground state in ^{188}Po. Preliminary evidence for this effect was recently suggested by an α-decay study [30].

5 Summary

Gamma rays from excited states of ^{190}Po have been identified using the RDT technique. From $I = 4\hbar$ onwards the

band behaves in a way similar to those observed in the isotones ^{188}Pb and ^{186}Hg, and is thus assigned a prolate-deformed configuration. This is the first case that a low-lying prolate configuration is observed in the polonium nuclei. From a VMI fit to the prolate states, the unperturbed prolate 0^+ state is estimated to lie at an excitation energy of only ~ 100 keV. Two-band mixing calculations predict the presence of a triplet of 0^+ states within an energy interval of ~ 100 keV only.

We are grateful to the $K = 130$ MeV cyclotron group for their excellent assistance. This work has been supported by the Academy of Finland under the Finnish Centre of Excellence Programme 2000-2005 (Project No. 44875, Nuclear and Condensed Matter Physics Programme at JYFL), the European Union Fifth Framework Programme "Improving Human Potential-Access to Research Infrastructure" (contract No. HPRI-CT-1999-00044), the FWO-Vlaanderen, the GOA (Onderzoeksprogramma K.U. Leuven), IUAP program (Belgium) and the Swedish Natural Research Foundation (NFR). K.V.d.V. is Research Assistant of the FWO-Vlaanderen. A.N.A. was partially supported by the EXOTAG project, HPRI-1999-CT-50017. M.B.S. was supported by the U.S. National Science Foundation.

References

1. F.R. May *et al.*, Phys. Lett. B **68**, 113 (1977).
2. A.M. Oros *et al.*, Nucl. Phys. A **645**, 107 (1999).
3. J.L. Wood *et al.*, Phys. Rep. **215**, 101 (1992).
4. R. Julin *et al.*, J. Phys. G **27**, R109 (2001); Eur. Phys. J. A **15**, 189 (2002).
5. N. Bijnens *et al.*, Phys. Rev. Lett. **75**, 4571 (1995).
6. N. Bijnens *et al.*, Phys. Rev. C **58**, 754 (1998).
7. N. Bijnens *et al.*, Z. Phys. A **356**, 3 (1996).
8. A.N. Andreyev *et al.*, J. Phys. G **25**, 835 (1999).
9. A.N. Andreyev *et al.*, Nature **405**, 430 (2000).
10. R.D. Page *et al.*, *Proceedings of the Third International Conference on Exotic Nuclei and Atomic Masses, Hämeenlinna, Finland, 2-7 July 2001* (Springer-Verlag, Heidelberg, 2003).
11. K. Helariutta *et al.*, Eur. Phys. J. A **6**, 289 (1999).
12. W. Satula, R. Wyss, Phys. Scr. T **56**, 159 (1995).
13. M. Leino *et al.*, Nucl. Instrum. Methods B **99**, 653 (1995).
14. H. Kettunen *et al.*, Acta Phys. Pol. B **32**, 989 (2001).
15. E.S. Paul *et al.*, Phys. Rev. C **51**, 78 (1995).
16. D. Alber *et al.*, Z. Phys. A **339**, 225 (1991).
17. L.A. Bernstein *et al.*, Phys. Rev. C **52**, 621 (1995).
18. W. Younes *et al.*, Phys. Rev. C **52**, R1723 (1995).
19. K. Helariutta *et al.*, Phys. Rev. C **54**, R2799 (1996).
20. N. Fotiades *et al.*, Phys. Rev. C **55**, 1724 (1997).
21. R.B. Firestone, *Table of Isotopes* (John Wiley & Sons, Inc., New York, 1996).
22. W. Younes, J.A. Cizewski, Phys. Rev. C **55**, 1218 (1997).
23. J.A. Cizewski, W. Younes, Z. Phys. A **358**, 133 (1997).
24. P. Magierski, R. Wyss, to be published.
25. J. Heese *et al.*, Phys. Lett. B **302**, 390 (1993).
26. R.V.F. Janssens *et al.*, Phys. Lett. B **131**, 35 (1983); W.C. Ma *et al.*, Phys. Rev. C **47**, R5 (1993).
27. M.A. Mariscotti *et al.*, Phys. Rev. **178**, 1864 (1969).
28. G.D. Dracoulis, Phys. Rev. C **49**, 3324 (1994).
29. R. Wyss, private communication (2003).
30. A.N. Andreyev *et al.*, Eur. Phys. J. A **6**, 381 (1999).